Energy Management Strategy of a Fuel Cell Electric Vehicle : Design and Implementation

Wahib Andari *‡, Aymen Khadrawi * , Samir Ghozzi*, Hatem Allagui *, Abdelkader Mami*

LAPER Research Unity (UR17ES11), Faculty of Sciences of Tunis, University of Tunis

El Manar2092 Tunis, Tunisia.

‡Corresponding Author:Wahib Andari , University of Tunis El Manar 2092 Tunis-Tunisia,

(andariwahib@yahoo.fr)

Received: 19.04.2019 Accepted:08.06.2019

Abstract- In this paper, we develop an energy management supervisor used to control power flow in a fuel cell electric vehicle, including a proton exchange membrane fuel cell and a supercapacitor. Our Target is to minimize the hydrogen consumption of a Proton Exchange Membrane (PEM) Fuel Cell. In order to perform this goal, the system is controlled through an Energy Management Strategy (EMS), to minimize the fuel cell power demand transitions and therefore improves its durability. The model of the studied system parts and the control strategy are developed using MATLAB software. Simulation results of our designed plan demonstrate a 40% gain in hydrogen consumption through the recovered energy from braking phases.

Keywords PEM Fuel Cell, Real Time , Power train , electric vehicle , Energy management , fuel consumption.

1. Introduction

These last few years, manufacturers of vehicles have taken an interest to overcome the significant environmental problems which caused mainly by conventional cars. In this context, Various energy generators have been developed based on renewable energy sources, such as solar, wind, hydraulic [1,2].At present, the development of Fuel cell electric vehicles (FCEV) represents one of the substantial topic challenges for scientists in many countries, owing to the energy supply problem and environmental problems [1,2,3].

However, In order to avoid more atmosphere pollution problems, The fuel cells (FC) represent one of the most promising renewable energy clean sources by generated only electricity, heat and water [4].There are various fuel cells technologies, the PEM fuel cell is the primary preference for the transportation area compared to other types of fuel cells, and offers a benefits such as the high power density, the working at a low temperature, and high efficiency [5].

Hence, these technologies raise the problem of limited power availability. Therefore, the idea of using an energy storage device with PEMFC energy sources, such as battery [6] or supercapacitor [7] was used to fulfill the fast load power demand and also to recover the energy from the braking phase [8,9,10]. Currently, the FCEV associated with several energy sources was the best solution which has been studied in numerous works such as [11,12] to ensure the power in the drive train and reducing the hydrogen consumption[13,14].For this reason, numerous researchers emphasize the importance of the power management strategy for FCEVs, which determines the power split between the FCS and a secondary power source.

In this respect, integrating a supervisory management strategy in such a system offers the opportunity to facilitate the control of energy flow to its interior as well as monitoring the operating status of its elements.

In recent literature, several management strategy approaches have been developed, which plays a crucial role in decreased fuel economy consumption considerably of powertrain performance [15].Among these techniques, equivalent consumption minimization strategy (ECMS) [16], rule-based algorithms [17], and fuzzy control logic [18] and dynamic Programming Approach [19].For this purpose, this paper aims to study and develop an energy management approach for FCEV vehicle system.

Hence, this paper expands the ideas of previous studies with a improvements regarding:

• An efficient design of FCEV with an energy management algorithm is proposed. Supercapacitor was included as a secondary source during the peak power.
• The adopted energy management is used to ensure power distribution flows between the different energy sources .and to provide a minimization of hydrogen consumption.

For that purpose, we will start in section 2 by modeling and sizing of the different used power sources separately: the PEMFC and the Maxwell supercapacitor. Next, we present in Section 3 the developed Buck/Boost converter. This converter is investigating the best power generation topology between supercapacitor and load. In section 4, we will propose an energy management strategy controlling the power demand between the different sources. Finally, we will conclude our work.

2. General Overview of the Studied System

The global system of the electric vehicle shown in fig.1 consists of two power sources: the first is composed by PEM fuel cell while the supercapacitor forms the second. For the functioning principle of the developed system, a Boost converter is utilized to connect the PEM fuel cell to DC bus voltage to obtain the desired output voltage.

On the other hand, A three-phase inverter supplying the power train. It is driven by a permanent magnet synchronous motor (PMSM).On the other side, a bidirectional buck/boost converter is used to interface the supercapacitor to DC voltage bus.

The studied system is controlled by a proposed energy management strategy which is developed to ensure and maintain excellent performance and high efficiency of the system by minimizing a hydrogen consumption of the fuel cell. For this purpose, the proposed EMS is used to compute the references power that must be delivered from each source according to the load power and the state of charge of a supercapacitor. Thus, this developed technique is composed of two controls blocks.

A working principle of each control blocks is to supervise the functioning of the primary and secondary energy sources related to it and receive the two references power ($P_{fuelcell-ref}$ and $P_{sc-ref)}$ generated from the developed energy management to control signals for each converter. The detailed schematic presented in Fig.8 shows the energy flow directions from each source based on two controls blocks, which are received a references power from the developed energy management approach.

A two controls blocks adopted for the developed system are detailed in Fig.3.
Where: d_{boost} : is the duty cycle for boost converter
d: is the duty cycle for buck/boost converter

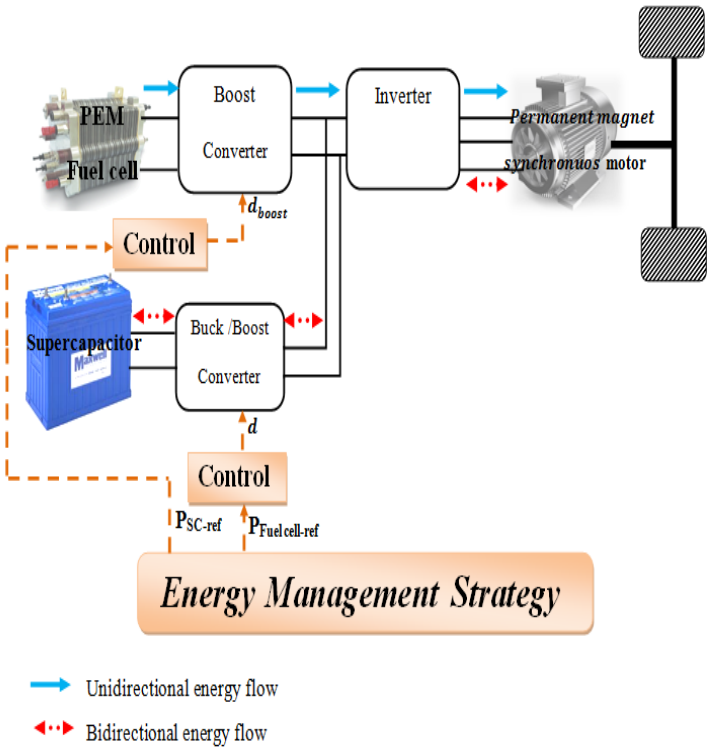

Fig.1. Descriptive schematic design of fuel cell / SC electric vehicle

2.1. Sizing Methodology

2.1.1. PEM Fuel cell sizing

Based on the works presented in [20], fig.2 is an equivalent presentation of a various irreversible loss mechanisms activation (V_{act}), concentration (V_{conc}) and ohmic over-voltages (V_{ohm}) causing voltage drops in a PEM Fuel Cell.

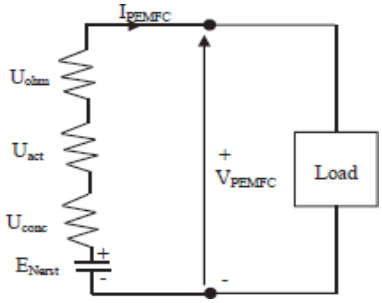

Fig. 2. PEMFC electrical circuit model.

Based on the given electrical circuit in Fig.2, the PEMFC's output voltage can be calculated as in (1)

$$V_{PEMFC} = E_{nerst} - V_{act} - V_{ohm} - V_{con} \quad (1)$$

Where :

E_{nerst} : theoretical potential of the cell

For this work, the nominal fuel cell power (P_{FC-nom}) is around 85kW . In addition, the auxiliary consumption varies from 15% to 20% of the nominal power[21]. In this case, The maximum Fuel Cell power is given by (2):

$$P_{FC-Max} = P_{FC-aux} + P_{FC-nom} = 102KW \quad (2)$$

The voltage cell limit (Ecell) is 0.7 V. This voltage considering the maximum power supplied by the fuel cell.

The FC exchanges voltage with the DC bus (V_{bus}) through a DC-DC boost converter. To obtain efficiency greater than 90 %, the adequate duty ratio is equals to 2.

Based on the works presented in [22], the fuel cell nominal voltage given by (3):

$$\frac{V_{bus}}{V_{FC-nom}} = 2 \Longrightarrow V_{FC-nom} = \frac{560}{2} = 280V \quad (3)$$

Then, the nominal current supplied by the FC is evaluated as:

$$I_{FC-nom} = \frac{P_{FC-max}}{V_{FC-nom}} = 364A \quad (4)$$

Finally , by considering the cell voltage E_{cell} = 0.7 V.The fuel cell must supply a 560 V DC bus via a Boost converter. Boost has a decreasing efficiency when the transformation ratio increases. So , the duty cycle must be around two for optimal operation.The number of cells combined in series ($N_{cell-serie}$) is calculated by the following equation (5):

$$N_{cell-series} = \frac{U_{DC}}{2.E_{cell}} = 400 \text{ Cell} \quad (5)$$

To summarize, the fuel cell parameters are shown in Table.1

Table 1. Characteristics of the studied Fuel cell

PEMFC parameters		
Stack power	Nominal	85KW
	Maximal	102KW
Nominal voltage		280V
Nominal current		300A
Number of cells		400cell
Temperature		368K
Air supply pressure		3bar
Fuel cell pressure		3bar

2.1.2. Supercapacitor Sizing Optimization

The supercapacitor (SC) is chosen as a second energy source in our study. This reversible power source presents a reliable solution to overcome the problems related to the operation of the PEMFC in order to ensure a fast response and the high power demands from the load during the transient phases [23].

The maximum power (P_{sc-max}) that the supercapacitor must provide to accelerate the vehicle from 0 to V_f = 90 Km/h at time t_a =14s is expressed as[23]:

$$P_{sc-max} = \frac{M}{t_a} V_f^2 \quad (6)$$

From equation (6), We have determined a maximum power P_{sc-max} = 100 kW.

The supercapacitor sizing methodology involves three steps described as follows :

The first step consists of determining the Maximum transfer energy of supercapacitor during acceleration phase ($E_{acc-max}$) . It is given by:

$$E_{acc-max}(w.h) = P_{sc-max}.t_a = 555.55w.h \quad (7)$$

Then, in the second step, we must determine the number of units of the supercapacitor. This case is divided into two parts: where the first is reserved to calculate the energy must be stored in supercapacitor to ensure the acceleration phase. It is calculated by (8) taking into account the state of charge (SOC) constraints [24]:

$$E_{uc-max} = \frac{E_{acc-max}}{SOC} = \frac{555.55}{0.6} = 925.91 \text{w.h} \quad (8)$$

The second part consists of determining the supercapacitor unit number. It is calculated by (9) taking into account the stored energy ($E_{uc,unit}$) given from the characteristics of supercapacitor presented in Table.2.

$$N_{uc} = \frac{E_{UC}}{E_{UC-unit}} = \frac{925.91}{2.33} = 397.38 \approx 398 \text{ units} \quad (9)$$

Finally, the last step consists in determining the number of cell in series (N_s) and parallel (N_p).For this N_S is calculated by (10)

$$N_s = \frac{U_{sc-max}}{V_{ele-max}} = \frac{360}{2.7} = 133.33 \approx 134 \quad (10)$$

And N_p is calculated by the following equation:

$$N_p = \frac{N_{uc}}{N_s} = \frac{398}{144} = 2.14 \approx 3 \quad (11)$$

To summarize, the supercapacitor battery on board the Electric vehicle (EV) consists of three blocks mounted in parallel. Each block contains 134 supercapacitor cells mounted in series. One cell capacity equal to 2700 F.

Table 2. Characteristic of the studied supercapacitor

Maxwell BOOSTCAP pc 2500	
Parameters	**Value**
Capacity , ($C_{uc,unit}$)	2700F
Rated voltage	2.5V
Maximal voltage	2.7V
Stored energy	8400J

Figure 3 is a detailed schematic that explains the working principle of the PEMFC/Supercapacitor controls structure.

The developed control for PEM fuel cell shown in fig.3.a is used to extract the maximum power from the fuel cell to overcome the demand power of the load during the different various driving cycle of the vehicle. In this work a simple PI controller is used to maintain a constant bus voltage of 560V in converter output, irrespective of variations in fuel cell voltage. The PI controller allows usefully comparing the reference and measured value of fuel cell current in order to minimize steady state error to zero. After that, PWM (Pulse Width Modulator) generator operates it will commute the MOSFET duty cycle.Also,based on the work in [25],a PI controller for hydrogen generated from the fuel cell is applied to control the delivered power.

Furthermore, to improve the robustness of the control strategy against the variations of power condition, the supercapacitor control is shown in fig.3.b is used to overcome the necessary power which is feeding the motor during the acceleration phase and overcome the needed power load demand variation when the available power of fuel cell is limited. Furthemore, the PI controller allows usefully comparing the reference and measured value of supercapacitor current according to eliminate the error and generated the desired response .Finally , a PWM signal is applied in order to control the eight switches (S_1,S_2,S_3,S_4,S_5,S_6,S_7,S_8) for buck/boost converter.

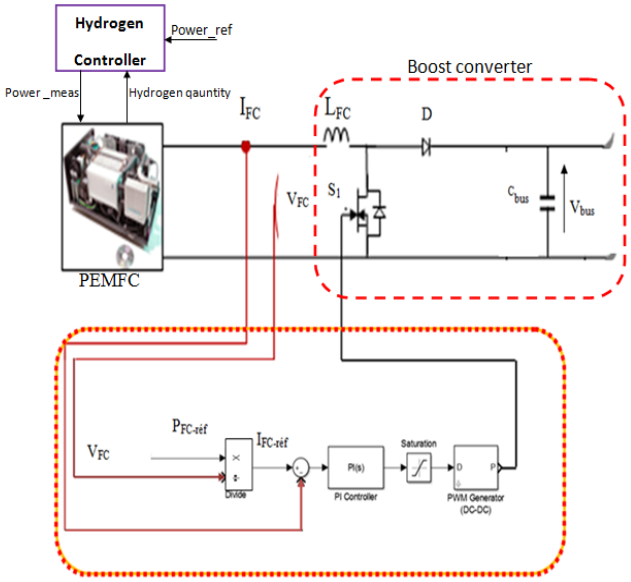

(a):PEMFC control

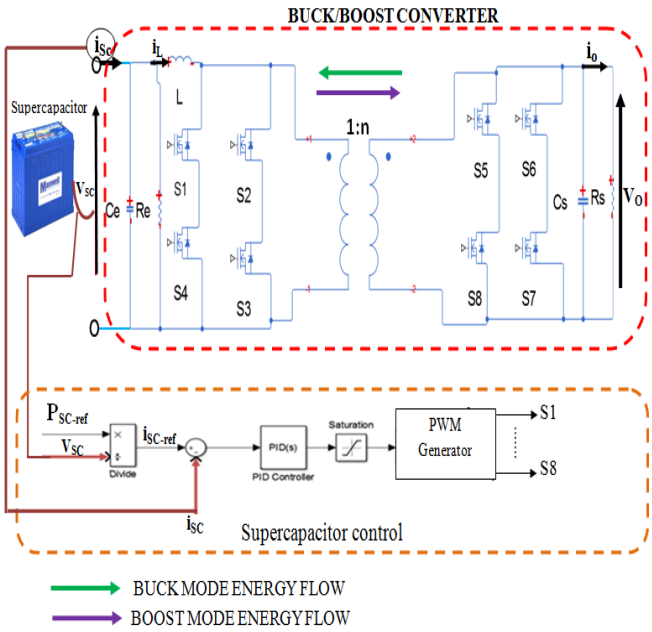

(b) : Supercapacitor control

Fig.3.PEMFC/Supercapacitor controls structure

The load power (P_{load}) of the vehicle is insured by using on traction forces needed during the acceleration phase, resistance forces and the required speed. It is modeled by the following equation [25]:

$$P_{load} = (F_{roll} + F_{aero} + F_{slope} + \frac{Md_v}{dt})V_{veh} \quad (12)$$

where :

F_{roll} is the Rolling resistance force. It is given as:

$$F_{roll} = M_{veh} g . f_r \quad (13)$$

F_{aero} is the aerodynamic drag force. Its expression is:

$$F_{aero}(t) = \frac{1}{2}\rho_{air} A_f C_x V_{veh}^2(t) \quad (14)$$

F_{slope} is the climbing force. It is given as :

$$F_{slope} = M_{veh} g \sin(\alpha(t)) \quad (15)$$

With: ρ_{air} is the air density, f_r is the resistance coefficient of the tire rolling A_f is the frontal surface area of the vehicle, $C_x$is the aerodynamic drag coefficient, M is the vehicle total mass, g is the gravity acceleration, α is the road slope angle.

Table 3 presents the parameters of the FCEV vehicle used for our study.

Table 3. Characteristics of the FCEV

Parameters	
Rolling resistance force f_r constant	$0.01 s2/m^2$

Air density	ρ_{air}	1.2kg/m^3
The frontal surface area of the vehicle	C_x	0.3
Aerodynamic drag coefficient	A_f	2.6m^2
Acceleration due to gravity	g	9.8m/s^2

3. Full Bridge Buck/Boost Converter

The full bridge buck/boost adopted for our work shown in fig.3.b allows the power flow between the power supercapacitor and the load. In applications such as: hybrid or electrical vehicles that transferred power is more than 750 watts, full bridge topology is a proper one [26,27,28].

It is composed of two full bridges, two planar transforms and eightswitchers MOSFETs (S_1,S_2,S_3,S_4,S_5,S_6,S_7,S_8).

The input side of the transformer is composed of four switches (S_1,S_2,S_3,S_4), input filter capacitor (C_e) and input resistor (Re).Then, the output side consisting of four switches (S_5, S_6, S_7, S_8),output filter capacitor (C_s) and output resistor (R_s).

3.2. Specific configuration

3.2.1. Boost mode

In the boost mode operation, the energy is transferred from the supercapacitor to the dc bus voltage. Hence,during this period, the secondary source will be supplied the motor.Figure 4presents the timing pulse conduction gating for the different switches (S_1,S_2,S_3,S_4) in boost mode operation.

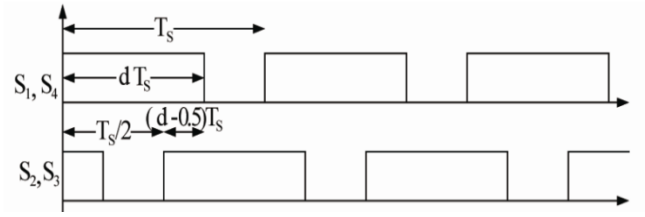

Fig.4. Boost mode conduction time for switches

The boost mode can be divided into two intervals, which are explained as follows :

Stage 1: This state lasts for (d – 0.5)Ts.

where: T_s is the switching period and d is the duty cycle.

During the first interval, the four switches (S_1,S_2,S_3,S_4) turn on. For this, the inductor voltage is equal to the input source.In this case, the planer transformer saves the power to transfer it in the second stage.

Therefore, the differential equations during this interval can be written as follows:

$$\frac{di_L}{dt} = \frac{V_{sc}}{L} \quad (16)$$

$$\frac{dV_o}{dt} = \frac{1}{C_s} i_o - \frac{V_o}{C_s R_s} \quad (17)$$

Stage 2 : This interval lasts for (1 – d)Ts . During The second state, the switchers (S1,S4) are on and the switchers (S_2 , S_3) are turned off .

This interval usually is known as the energy transfer interval. In this case, the supercapacitor is discharged in the load through the planar transformers and both switches (S_1,S_4)

For this, the output state in this interval can be expressed as follows:

$$\frac{di_L}{dt} = \frac{V_o}{nL} + \frac{1}{L} V_{sc} \quad (18)$$

$$\frac{dV_o}{dt} = \frac{i_L}{nC_s} - \frac{-1}{C_s R_s} V_o + \frac{i_o}{C_s} \quad (19)$$

where: n is the turn ratio of a transformer

3.2.2.buck mode

In the buck mode operation, the power flow from the load to the supercapacitor. Therefore, the secondary source is in the recharge mode. The control signals for different switches (S_5,S_6,S_7,S_8) in buck mode operation are shown in fig.5.

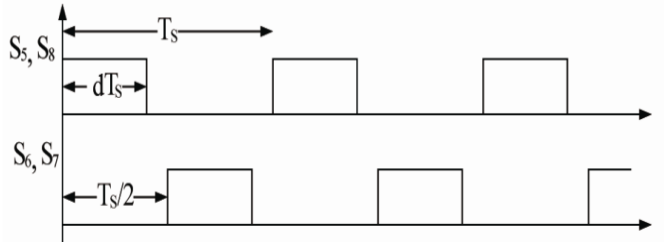

Fig.5. Buck mode conduction time for switches

Moreover, two main operating intervals are considered to illustrate circuit conditions. The behavior of this state will be described below :

Stage 1: This interval lasts for dTs. During the first state, the switches (S_6,S_7) are conducting and the switchers (S_5, S_8) are turned off.

In this case, the power circulates from the load to capacitors through transformers.The following equations describe thebehavior of this state:

$$L\frac{di_L}{dt} = \frac{V_o}{n} - V_{SC} \quad (20)$$

$$\frac{dV_{SC}}{dt} = \frac{-1}{C_E} i_L - \frac{-1}{C_E R_E} V_{SC} + \frac{i_o}{C_E} \quad (21)$$

Stage 2: This state lasts for (0.5 – d)Ts.During the second interval, the four switches (S5,S6,S7,S8) turn off. The inductor voltage is equal to the input source. In this case, the secondary side is only fed by the inductor stored power.

The equations during this interval can be expressed as follows:

$$\frac{di_L}{dt} = \frac{V_o}{L} \quad (22)$$

$$\frac{dV_{SC}}{dt} = \frac{1}{C_E} i_o - \frac{V_{SC}}{C_E R_E} - \frac{1}{C_E} i_L \quad (23)$$

Based on the work presented in [29],equations (24-25) give the stator voltages and electromagnetic torque of the permanent magnet synchronous (PMSM) in d-q reference.

$$\begin{cases} V_{ds} = R_s i_{ds} + L_{ds} \frac{di_{ds}}{dt} - \omega L_{qs} i_{qs} \\ V_{qs} = R_s i_{qs} + L_q \frac{di_{qs}}{dt} + \omega (L_{ds} i_{ds} + \varphi_f) \end{cases} \quad (24)$$

The electromagnetic torque can be expressed as:

$$C_{em} = \frac{3}{2} p[(L_{ds} - L_{qs}) i_{ds} i_{qs} + i_{qs} \varphi_f \quad (25)$$

Where :

V_{ds},V_{qs} are the stator voltages on d and q axes

i_{ds}, i_{qs} are the components of the current respectively on d and q axes

R_s, L_{ds} are the stator winding resistance and inductance, p is the number of pole pairs

φ_f is the permanent magnetic flux

4. Energy Management Approach Developed

The energy flows between the load and the power sources are distributed by the energy management algorithm in order to optimize the hydrogen consumption during the various driving phases such as : acceleration ,deceleration and stopping phases.

In literature, several types of power management strategies have been developed to improve the fuel economy of FCEV [30] such as optimal control [31,32], rule-based algorithms [33] and fuzzy logic [34]. In this context, the developed energy management algorithm in our work taking into account the variation of load power (P_{load}) and the state of charge of supercapacitor (SOC) in a way to minimizes the hydrogen consumption. Thus, The load power (P_{load}) is according to the relationship given by (26):

$$P_{load} = P_{fuel-cell} + P_{SC} \quad (26)$$

The proposed technique is detailed and explained in fig.6.

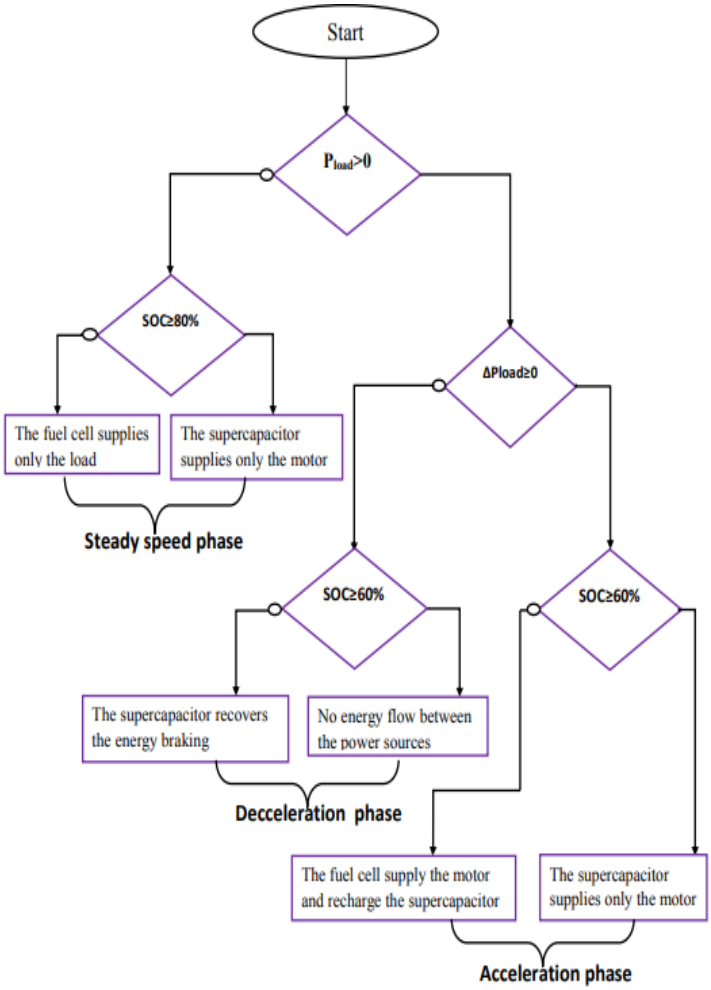

Fig.6. Flowchart of energy management algorithm

5. Simulation Results and Discussion

This section is devoted to test and evaluate the efficiency of the developed energy management approach for fuel cell electric vehicle system. Thus, we present some simulation results in Figs. 7-12 which are obtained by considering the energy management approach.

In this case, We have chosen a profile speed (Fig. 7) applied to the FCEV system during 100s and as 50Km/h maximum speed.

Based on the drive cycle profile, We notice three primaryoperating modes are represented in Fig. 7 are set as next:

Mode 1: Traction mode.

Mode 2: Steady speed phase.

Mode 3: Braking mode.

Furthermore, based on different working mode of the vehicle, the obtained results are shown in Fig 9 - 11 which represent the state of charge of the supercapacitor, the power delivered respectively by a supercapacitor and a fuel cell. The different modes are explained as next:

Mode 1: During the starting phase of the vehicle from 0 to40 s, the system runs on accelerationmode. In this case, the fuel cell was turned off and the supercapacitor should be discharged and delivers its power to the load (SOC≥ 60%)(Fig.10).

Mode 2: The vehicle is in steady speed state mode from the 40s to 70s.At this moment, The power demand by the powertrain is provided by the fuel cell and the secondary power source is considered off (SOC<80%).In this context, the power required by the powertrain based on PMSM is supplied only by the fuel cell.(Fig.11)

Mode 3: The system operates in mode three during the remaining period from 70 to 100 s.During this last phase, the vehicle is in braking mode and the fuel cell was turned off. In this case,thesupercapacitor receives power from the braking phase (Fig.10).

Figure.8 illustrates the obtained result of the power delivered by the powertrain (P_{load}). This available power is according to the relationship given by (26). It's remarkablethat the supercapacitor supplies the load under braking and traction phases, but the fuel cell supplies it's at steady states speed.

Figure 12 illustrates the hydrogen consumed by the fuel cell alone without energy management algorithm. There is a maximum consumption 15g /s when the maximum speed of the cycle is reached 50 km/h at time 70 s.

Hence, The hydrogen consumed when the proposed energy management algorithm is implemented shown in fig.13. The quantity of hydrogen consumption obtained is around 9g/s. By comparing the hydrogen consumption in the two presented cases, the hydrogen consumption decreases from 15g to 9g. It is clear that the hydrogen consumption obtained by the proposed algorithm is minimized by 6g.

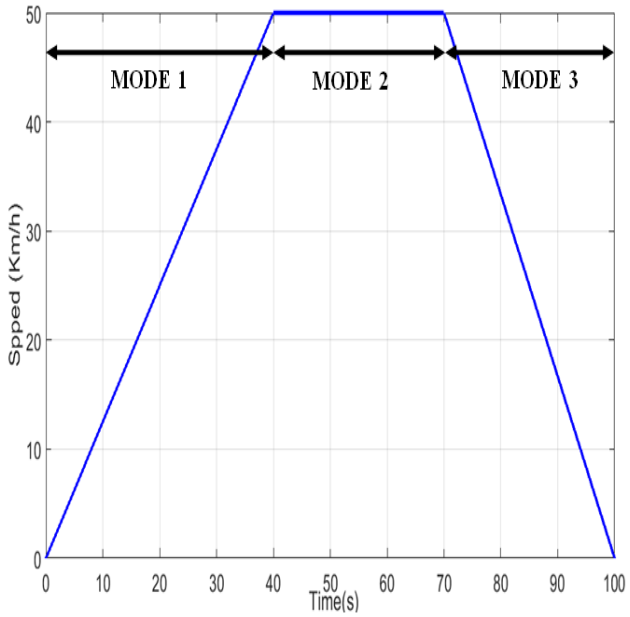

Fig. 7. Speed profile

As we can see, thedevelopedenergy managementhas guaranteed a 40 % gain in hydrogen consumption.

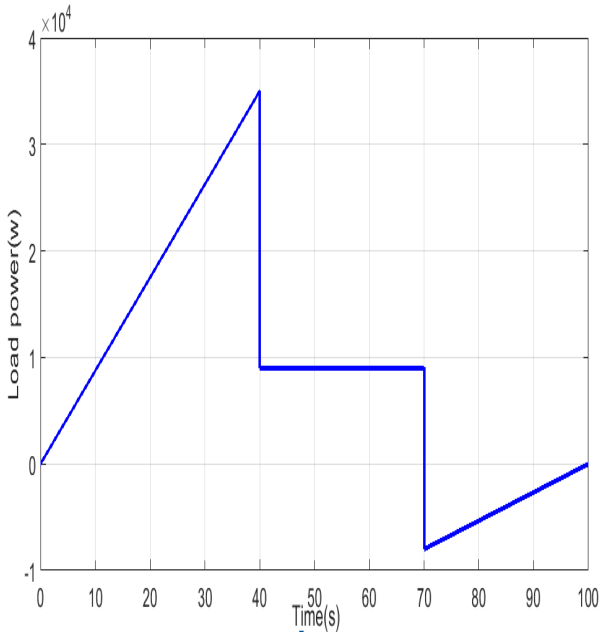

Fig.8. The load power

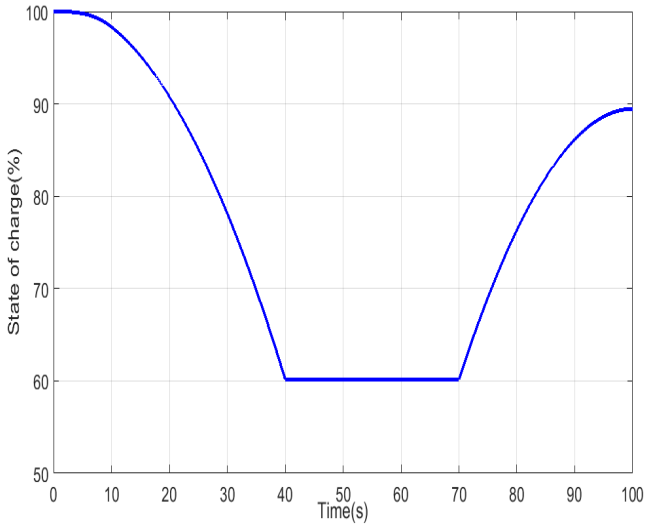

Fig. 9.State of charge(SOC)

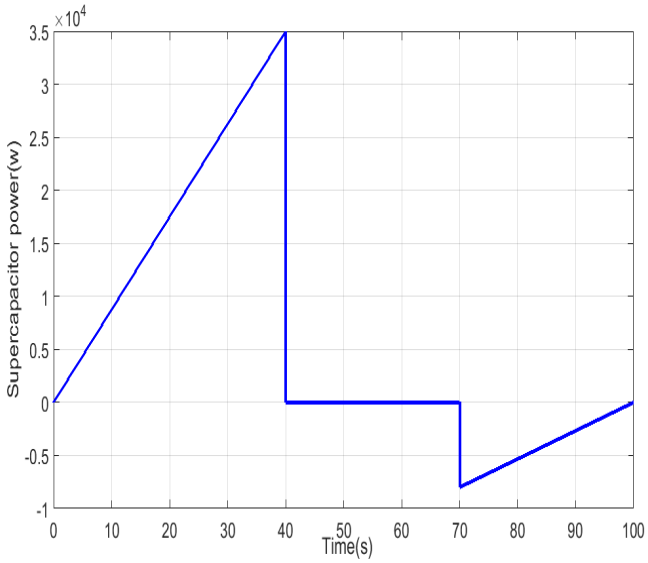

Fig.10. Reference supercapacitor power

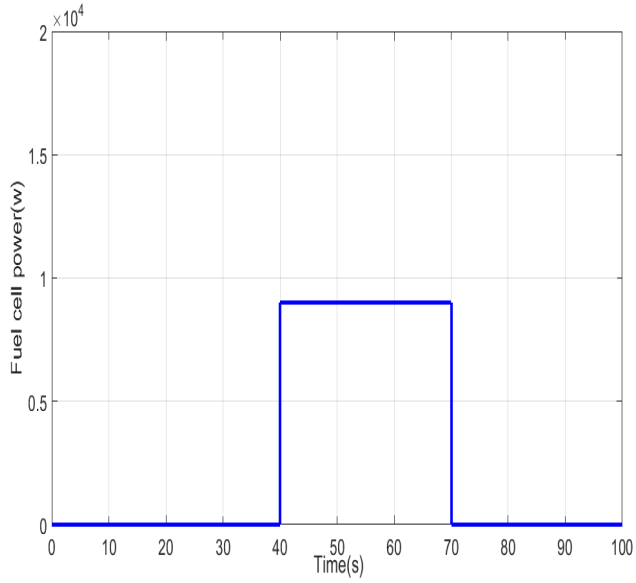

Fig.11. Reference fuel cell power

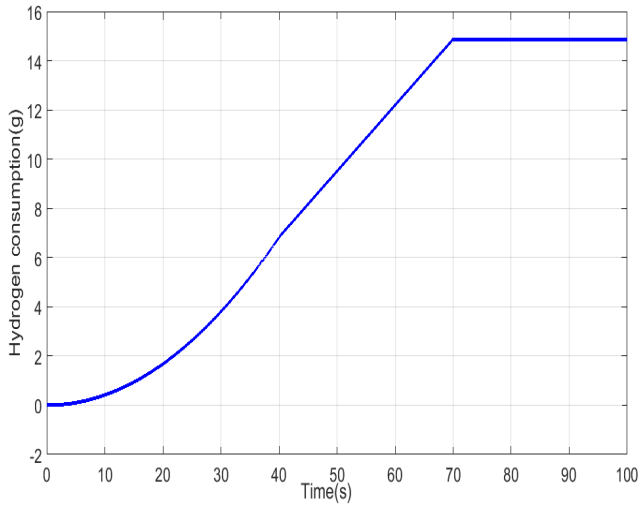

Fig. 12. Hydrogen consumption with our energy management algorithm

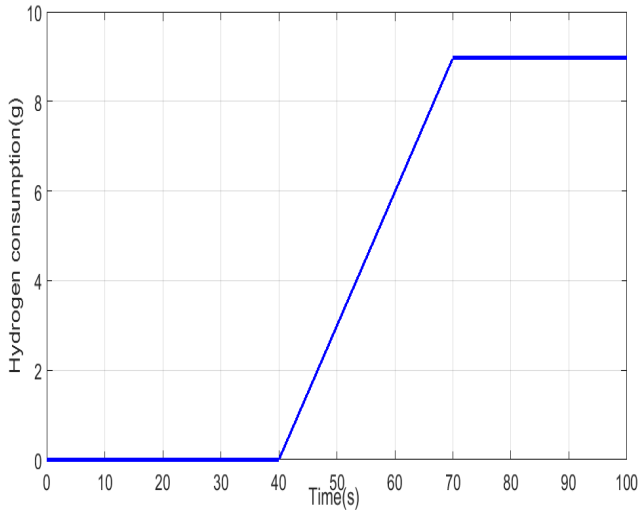

Fig. 13. Hydrogen consumption with an energy management algorithm

Then, in order to validateand prove the effectiveness of the developed energy management approach and to performit on real-time implementation, we have implemented the developed approach on STM32F4 Board.

In this context, the PIL (processor in the loop) is the fundamental method for the plan to test the implementation of our EMS [35].For that purpose, the PIL process means that the energy management algorithm is modeled and developed viafour following steps are set as next : (Fig.14)

In the first step, the plant model will be simulatedon the host computer using Matlab/Simulink. After automatically compiling, the developed energy management approach is quickly loaded on the STM32 Discovery F4 microcontroller to create the PIL block.Moreover, the communication between the STM32F4 board and the computer is ensured by ST-LINK communication.

Next, A code generation by the STM32F4 discovery board from the model by using the PIL process.

Consequently, this hex file code generated which will be run in the microcontroller embedded board while the plant model will be simulated in the host computer.

Then,Simulink and embedded target will run at the same time and will exchange available data based on the energy management approach implemented by the PIL block process (Fig.15).

Finally, we can analyze the real-time resultsusing Matlab/Simulink.

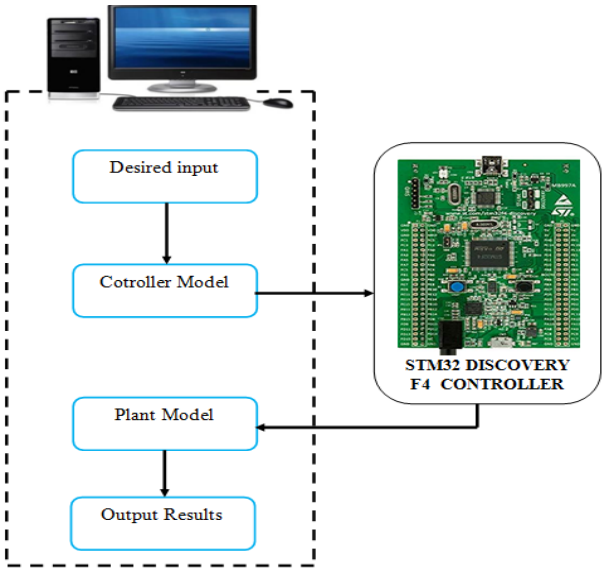

Fig .14 Simulink Prototype

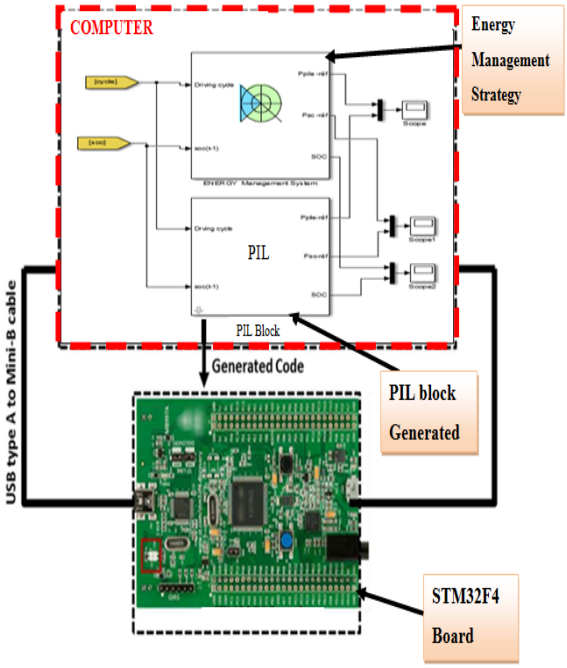

Fig .15 The energy management system using the PIL block.

After the energy management approach was designed and implemented, Fig. 16and 17 illustrate respectively, the real-time results of reference powers for fuel cell ($P_{fuel\ cell\text{-}ref}$) and a supercapacitor ($P_{sc\text{-}ref}$).

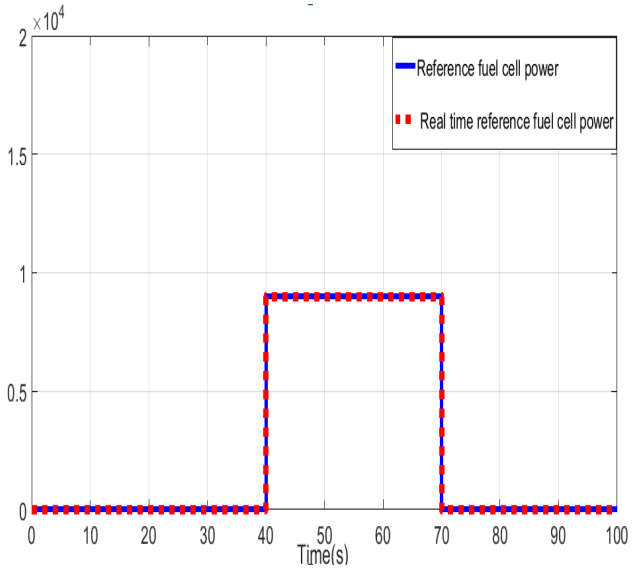

Fig.16. Real-time reference fuel cell power

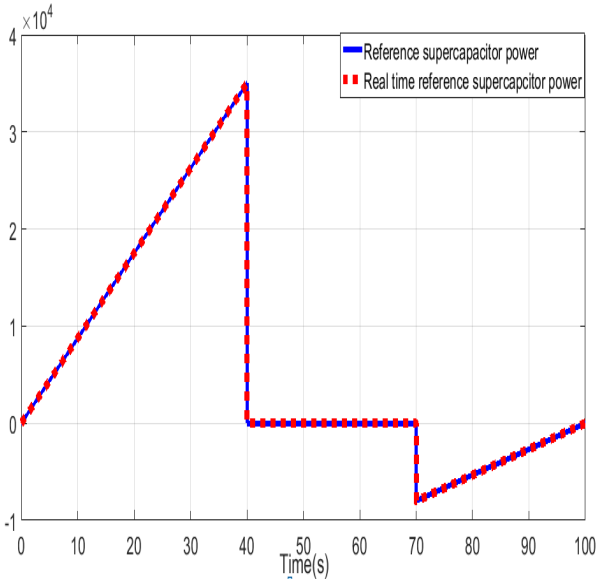

Fig.17 Real-time reference fuel cell power

As we can notice, there is an agreement between the simulation results of the developed energy management and real-time results performed, which confirms that the implemented EMS is robust and reliable.

Therefore, the PIL process can be used as a low-cost solution to test the hardware implementation of the proposed energy management approach.

6. Conclusion

In this work, an energy management approach was presented and used to analyze the dynamic performance and power distribution for the FCEV system. The different parts of the proposed system have been simulated separately and

the energy management has been used to coordinate between the various sources in a way to supply the PMSM. Thanks to this proposed technique, the obtained results has successfully achieved the desired working performance of the system by minimizing the hydrogen consumption of the fuel cell du a braking energy recovery by a supercapacitor. Experiment results validated this approach.

References

[1] A.Hassoune et al.,"Power Management Strategies of Electric Vehicle Charging StationBased Grid Tied PV-Battery System", International Journal of Renewable Energy Research, vol. 8(2), 2018.

[2] Sushil Kumar, B.; Krithiga, S.; SarathiSubudhi, P. Wireless Electric Vehicle Battery Charging System using PV Array. Indian J. Sci. Technol. 2016, 9, 1–5.

[3] Michela Longo; Wahiba Yaïci ; Federica Foiadelli ;" Electric vehicles charged with residential's roo f solar photovoltaic system : A case study in Ottawa ", IEEE 6th International Conference on Renewable Energy Research and Applications (ICRERA), 121 - 125, 2017.

[4] Wahib Andari, Samir Ghozzi, Hatem Allagui and Abdelkader Mami, "Design, Modeling and Energy Management of a PEM Fuel Cell / Supercapacitor Hybrid Vehicle" International Journal of Advanced Computer Science and Applications(ijacsa), Vol.8(1), 2017.

[5] Salsabil Gherairi, Hybrid Electric Vehicle: Design and Control of a Hybrid System (Fuel Cell/Battery/Ultra-Capacitor) Supplied by Hydrogen 1,2 Energies 2019, vol. 12(7), 1-19, 2019.

[6] Savvas Tsotoulidis, Athanasios Safacas, "Analysis of a Drive System in a Fuel Cell and Battery powered Electric", International Journal of Renewable Energy Research, vol. 1(3), 2011.

[7] Mahdiyeh Khodaparastan , Ahmed Mohamed ,"Supercapacitors for electric rail transit systems ", International Conference on Renewable Energy Research and Applications (ICRERA) , 2017.

[8] Bianchi F, Ocampo-Martinez C, Kunusch C, Sanchez- Pena R. , "Fault-tolerant unfalsified control for PEM fuel cell systems", IEEE Trans Energy Convers ,Vol.30(1),1-9, 2015.

[9] Poria Fajri ; Shoeib Heydari ; Nima Lotfi , " Optimum low speed control of regenerative braking for electric vehicles ", IEEE 6th International Conference on Renewable Energy Research and Applications (ICRERA) , 875 – 879,2017.

[10] Ismail Oukkacha, Mamadou Baïlo Camara , Brayima Dakyo,"Electric vehicles energy management using direct torque control space vector pulse width modulation combined to polynomial controllers", IEEE 6th International Conference on Renewable Energy Research and Applications (ICRERA) ,473 – 478, 2017.

[11] Erdinc O, Vural B, Uzunoglu M, Ates Y," Modeling and analysis of an FC/UC hybrid vehicular power system using a wavelet fuzzy logic based load sharing and control algorithm", Int J Hydrogen Energy,Vol.34(52), 23-33, 2009

[12] Hosseinzadeh E, Rokni M, Advani Suresh G, Prasad Ajay K," Performance simulation and analysis of a fuel cell/battery hybrid forklift truck", Int J Hydrogen Energy,Vol.38(4), 1-9, 2013

[13] WahibAndari , Samir Ghozzi , HatemAllagui , Abdelkader Mami ,"Optimization of Hydrogen Consumption for Fuel Cell Hybrid Vehicle", indian journal and science Vol. 11(2), 2018.

[14] Kim NW, Cha SW, Peng H," Optimal control of hybrid electric vehicles based on Pontryagin's Minimum Principle", IEEE Trans Control Syst Technol,Vol.19(12) ,79-87, 2011

[15] Harun TURKER, SeddikBacha, "Smart Charging of Plug-in Electric Vehicles (PEVs) in Residential Areas: Vehicle-to-Home (V2H) and Vehicle-to-Grid (V2G) ", International Journal of Renewable Energy Research, Vol. 4(4), 2014.

[16] Xu LF, Li JQ, Hua JF, Li XJ, Ouyang MG, "Optimal vehicle control strategy of a fuel cell/battery hybrid city bus", Int J Hydrogen Energy; Vol. 34(73), 23-33, 2009

[17] Ehsani M, Gao YM, Emadi A, "Modern electric, hybrid electric, and fuel cell vehicles",2nd ed. Boca Raton: CRC pres, 2010.

[18] N. Al-Rousan Mohammad Al-Rousan Adnan Shariah , " A fuzzy logic model of a tracking system for solar panels in northern Jordan based on experimental data", International conference on Renewable Energy Research and Applications (ICRERA), 2012 .

[19] Chaofeng Pan , Yanyan Liang , Long Chen and Liao Chen, " Optimal Control for Hybrid Energy Storage Electric Vehicle to Achieve Energy Saving Using Dynamic Programming Approach", Energies 2019, Vol. 2(4), 1-19, 2019.

[20] Houssem CHAOUALI, Wafa Ben SALEM, Dhafer MEZGHANI, Abdelkader MAMI, "Fuzzy Logic Optimization of a Centralized Energy Management Strategy for a Hybrid PV/PEMFC System Feeding a Water Pumping Station", International Journal of Renewable Energy Research, Vol. 7(3), 2017.

[21] Allaoua Bet al, "Energy management of PEM fuel cell/ supercapacitor hybrid power sources for an electric vehicle ", Int J Hydrogen Energy; Vol. 2(5), 1-14, 2017.

[22] Islem Lachhab, LotfiKrichen, , " Impact of Ultra-Capacitor Sizing Optimization on Fuel Cell Hybrid Vehicle ", International Journal of Renewable Energy Research, Vol 5 (1), 2015.

[23] Damith B. Wickramasinghe Abeywardana ; Branislav Hredzak ; Vassilios G. Agelidis, " Battery-supercapacitor hybrid energy storage system with reduced low frequency input current ripple", International Conference on Renewable Energy Research and Applications (ICRERA) , 328 - 332 , 2015

[24] M. Uzunoglu, M.S. Alam, "Dynamic modeling, design and simulation of a PEM fuel cell/ultracapacitor hybrid system for vehicular applications", *Energy Conversion and Management,* 1544–1553, 2007.

[25] R. Govindarasu, R. Parthiban, P.K. Bhaba ,“ Investigation of Flow Mal-distribution in Proton Exchange Membrane Fuel Cell Stack”, *International Journal of Renewable Energy Research*, Vol. 2(4), 2012.

[26] Shahab H. A. Moghaddam, Ahmad Ayatollahi, AbdolrezaRahmati, “ Modeling and Current Programmed Control of a Bidirectional Full Bridge DC-DC Converter ”, *Energy and Power Engineering*, Vol.4(2), 2012.

[27] Yuki Iwata ; Kazuma Suzuki ; Takaharu Takeshita ; Yuji Hayashi ; Seiji Iyasu ,“Isolated bidirectional singlephase AC/DC convert er using a soft switching technique”, IEEE 6th International Conference on Renewable Energy Research and Applications (ICRERA), 383 - 388, 2017.

[28] Enes Ugur; Bulent Vural ,“ Comparison of different small signal modeling methods for bidirectional DC-DC converter ”, International Conference on Renewable Energy Research and Application (ICRERA) , 913 - 915 , 2014.

[29] Xiaoquan Lu ; Heyun Lin ; Yi Feng ; Yujing Guo ; Hui Yang , “ Improvement of sliding mode observer for PMSM sensorless control in renewable energy system ”, International Conference on Renewable Energy Research and Applications (ICRERA), 769 - 77 , 2013.

[30] Mamadou Lamine Doumbia ,“ PEM Fuel Cell Modelling Using Artificial Neural Networks”, International Journal of Renewable Energy Research, Vol 4(3), 2014 .

[31] G. Paganelli, T.M. Guerra, S. Delprat, J.J. Santin, M. Delhom, E. Combes, “ Journal of Automobile Engineering”, Vol.214 (7), 705–718, 2000

[32] Bala Murugan, Manoharan S Optimal Power Flow Management Control for Grid Connected Photovoltaic/Wind turbine/Diesel generator (GCPWD) Hybrid System with Batteries ”, International Journal of Renewable Energy Research ,Vol 3(4) ,2013.

[33] Ansarey M, Panahi MS, Ziarati H, Mahjoob M, “Optimal energy management in a dual-storage fuel-cell hybrid vehicle using multi-dimensional dynamic programming, J Power Sources, Vol. 12(2), 59-71, 2014.

[34] Brahma A, Guezennec Y, Rizzoni G, “ Optimal energy management in series hybrid electric vehicles, American Control Conference, vol(11). p. 1-8, 2000.

[35] Ben Slama Sami , Nasri Sihem , ZafarBassam “Design and implementation of an intelligent home energy management system: A realistic autonomous hybrid system using energy storage”, Int J Hydrogen Energy,Vol. 2(5), 1-14, 2018.